

Predicting reach-specific properties of fluvial terraces to guide future fieldwork. A case study for the Late Quaternary River Allier (France) with the FLUVER2 model

Tom Veldkamp,^{1*} Jeroen M. Schoorl² and Willem Viveen³

¹ Faculty of Geo-Information Science and Earth Observation (ITC), University of Twente, P.O. Box 217, 7500 AE Enschede, The Netherlands

² Soil Geography and Landscape group, Wageningen University, P.O. Box 47, 6700 AA Wageningen, The Netherlands

³ Sección Ingeniería de Minas e Ingeniería Geológica, Departamento de Ingeniería, Pontificia Universidad Católica del Perú, San Miguel, Lima, Perú

Received 7 February 2016; Revised 22 August 2016; Accepted 22 August 2016

*Correspondence to: Tom Veldkamp, Faculty of Geo-Information Science and Earth Observation (ITC), University of Twente, P.O. Box 217, 7500 AE Enschede, The Netherlands. E-mail: a.veldkamp@utwente.nl

[Correction added on 20 October 2016 after first online publication: The author name Willem Viveen was incorrect and has been corrected in this version.]

ESPL

Earth Surface Processes and Landforms

ABSTRACT: Numerical models have not yet systematically been used to predict properties of fluvial terrace records in order to guide fieldwork and sampling. This paper explores the potential of the longitudinal profile model FLUVER2 to predict testable field properties of the relatively well-studied, Late Quaternary Allier system in France. For the Allier terraces an overlapping ¹⁴C and U-series chronology as well as a record of ¹⁰Be erosion rates exist. The FLUVER2 modelling exercise is focused on the last 50 ka of the upper Allier reach because for this location and period the constraints of the available dating techniques are tightest. A systematic calibration based on terrace occurrence and thicknesses was done using three internal parameters related to (1) the sediment erodibility; (2) the sediment transport distance; and (3) the sediment supply derived from the surrounding landscape. As external model inputs, the best available, reconstructed, tectonic, climatic and base-level data were used. Calibrated model outputs demonstrate a plausible match with the existing fluvial record. Validation of model output was done by comparing the modelled and measured timing of aggradation and incision phases for the three locations. The modelled range of landscape erosion rates showed a reasonably good match with existing erosion rate estimates derived from ¹⁰Be measurements of fluvial sands. The quasi-validated model simulation was subsequently used to make new testable predictions about the timing and location of aggradation and erosion phases for three locations along the Allier river. The validated simulations predict that along the Allier, reach-specific dynamics of incision and aggradation, related to the variations in sediment supply by major tributaries, cause relevant differences in the local fluvial terrace stratigraphy. Copyright © 2016 John Wiley & Sons, Ltd.

KEYWORDS: terrace; numerical model; Quaternary; erosion rate; field work

Introduction

Fluvial terraces are often studied by means of field mapping of geomorphological and sedimentological characteristics (Bridgland and Westaway, 2008; Maddy *et al.*, 2012; Stokes *et al.*, 2012; Cordier *et al.*, 2014). These studies provide geologists with conceptual models of palaeo-conditions especially when they are combined with radiometric and fossil-based dating of selected sediment samples. Fluvial terraces are less commonly studied by means of computer simulations and only a few numerical landscape evolution models are able to produce fluvial terraces, and so far none has been able to produce a complete terrace staircase and/or stratigraphy (Coulthard *et al.*, 2002; Gargani *et al.*, 2006; Wainwright, 2006; Tucker and Hancock, 2010; Coulthard and van de Wiel, 2013; Geach *et al.*, 2015; Briant *et al.*, 2016; Temme *et al.*, 2016).

Because the fluvial terrace studies usually start with a set of terraces as a given, they tend to neglect locations with limited or nonexistent archives. With fluvial terraces specifically this is important as they represent, by default, an incompletely preserved record that only partially recorded environmental change (Cordier *et al.*, 2014). By focusing on what is still preserved, field work might systematically be biased towards settings which might not be generally representative. This bias might even be enhanced because often studies are focused on the most elaborate and accessible exposures often provided by gravel and sand pits. These man-made exposures are only made at locations where the thickest deposits occur, again potentially creating a systematic bias in the observation locations. A clear example is provided by the Mino system, where gravel pits are mainly found in local relatively subsiding basins (Viveen *et al.*, 2014).

Instead of letting available outcrops guide study and sample locations we could also attempt to get a more balanced overall system approach using numerical modelling. Calibrated models should be able to indicate where and when fluvial records were created and what conditions they represent. Although existing numerical models have severe limitations they can provide a general overview of past events including the locations and ages of potential records (Briant *et al.*, 2016; Temme *et al.*, 2016). Unfortunately they are still unable to provide estimates of preservation. This implies that a modelling exercise could potentially guide future fieldwork to locations with specific hypothesis about the potentially available fluvial record.

In this paper we explore if this alternative way of guiding future field work is already feasible for a relatively well investigated system (Upper Allier system).

A simple, longitudinal profile model specifically designed to support fluvial terrace studies is the FLUVER2 model (Veldkamp and van Dijke, 1998, 2000). This model, classified as a 'spatially lumped model' by Temme *et al.* (2016), describes fluvial system development along a longitudinal profile by simulating vertical erosional and depositional events as a function of climate, base-level and tectonic temporal changes. Spatially lumped models are often used to model fluvial landscape dynamics at glacial–interglacial timescales using reduced-complexity modelling approaches (Gasparini *et al.*, 2006; Viveen *et al.*, 2013; Forzoni *et al.*, 2014; van Gorp *et al.*, 2015). Although there are concerns about their suitability for landscape evolution modelling (Tucker and Hancock, 2010), these models have proved their value despite known limitations such as the inability to simulate terrace preservation and to produce realistic landscapes. Most landscape reconstructions based on numerical modelling techniques have been made by simplified reduced complexity models (Temme *et al.*, 2016 and references within).

FLUVER2 generates a record of potential terrace forming events, which are defined as a floodplain aggradation phase followed by a floodplain incision phase. In most applications of the model the emphasis has been on obtaining a match with known field records to learn about the relative controls of external driving forces (climate, base-level and tectonics) on terrace formation (Tebbens *et al.*, 2000; Veldkamp *et al.*, 2002; Stemerding *et al.*, 2010; Viveen *et al.*, 2013; Geach *et al.*, 2015).

Every fluvial system model requires data on initial conditions and realistic temporal inputs that allow a measure of calibration with known field records. Under the best possible circumstances quasi-validations might be possible (Oreskes *et al.*, 1994). Often models are calibrated on known field data to obtain plausible erosion and/or sedimentation dynamics. Subsequently, several scenarios are constructed and simulated, followed by a discussion on the merit of specific scenario assumptions (Gasparini *et al.*, 2006; Van Balen *et al.*, 2010; Whittaker and Boulton, 2012; Stange *et al.*, 2016).

Attempts to validate landscape models are rare (Sapozhnikov *et al.*, 1998) and only one example of a quasi-validation exists for the FLUVER2 model, namely for the Meuse system. The model was first calibrated on terrace altitudes and reconstructed erosional and depositional dynamics (Tebbens *et al.*, 2000). However, the inclusion of sediment composition in the calibrated version using (i) source area composition and (ii) sediment supply and mixing, generated a sediment-compositional-change curve for each modelled reach of the Meuse River through time. This synthetic curve of an independently generated parameter demonstrated a good match with a field-measured, geochemical sediment composition curve of overbank deposits (Tebbens and Veldkamp, 2000), yielding a quasi-validation for this calibrated model version.

Most modelling exercises include sensitivity analyses (Tebbens and Veldkamp, 2001; Geach *et al.*, 2015). For many short-term (decadal) or event-driven landscape evolution models such as LAPSUS and OpenLISEM, Monte Carlo simulations based on measured frequencies and probabilities is a common approach (Temme *et al.*, 2011; Baartman *et al.*, 2013). Like other lumped models, FLUVER2 has also lumped time steps (in this case 20 years) making this model less suitable for Monte Carlo sensitivity analysis using historical data.

More often models are illustrated by demonstrating model behaviour when model settings are systematically changed. (Veldkamp and Tebbens, 2001; Van Balen *et al.*, 2010; Schoorl *et al.*, 2014). Such exercises have, for example, demonstrated that fluvial terraces are diachronous features as the timing of their formation migrates along the profile (Tebbens and Veldkamp, 2001). This nonlinear behaviour is more pronounced in the downstream reaches, where base-level changes directly or indirectly affect terrace formation depending on whether the continental shelf is narrow (Schumm, 1993; Blum and Törnqvist, 2000; Viveen *et al.*, 2013). In the upper reaches terrace formation events are often temporary features due to the steep slopes, limited amounts of sediments and the fast migration of sediment pulses followed by complex-response incision (Schumm, 1977), demonstrated in detail for a decadal LAPSUS case study for Spain (Schoorl *et al.*, 2014). The impact of fast and gradual changes in climate and base-level changes was explored with elaborate numerical modelling experiments demonstrating that, except for the headwaters where usually no record is preserved, no straightforward relationship exists between climate, base-level, crustal uplift inputs and terrace formation (Tebbens *et al.*, 2000; Stemerding *et al.*, 2010).

There are seven independent FLUVER2 applications, all concerning western and southwestern European rivers systems: the Allier–Loire in France (Veldkamp and van Dijke, 1998), The Meuse in the Netherlands (Tebbens *et al.*, 2000), the Aller (Weser tributary) in Germany (Veldkamp *et al.*, 2002), the Guadalhorce in southern Spain (Schoorl and Veldkamp, 2003), the Thames in England (Stemerding *et al.*, 2010), the Miño in Portugal and Spain (Viveen *et al.*, 2013), and the Tabernas in south-eastern Spain (Geach *et al.*, 2015). The results of these modelling exercises have mainly been used to gain insight to the plausibility of specific external controls and relationships between external drivers and terrace formation. They also helped to understand for example why specific terrace correlations are difficult or uncertain (Veldkamp *et al.*, 2002; Viveen *et al.*, 2013).

Briant *et al.* (2016) propose a clearer separation between field data used for model specification (input data) and that used for evaluation (output data). They also propose a wider range of data to be used in model evaluations. We will follow this recommendation and focus less on testing fieldwork-derived hypotheses with respect to external controls and instead focus more on making testable location specific field predictions based on calibrated and validated model simulations. We will use the whole loop of field and model data use as proposed by Temme *et al.* (2016) in their Figure 5. They identify data used to run the model (input and parameterisation data), data used to learn about the model (calibration and validation data) and finally model data to make field predictions.

Our paper will describe a FLUVER2 modelling exercise focusing on the last 50 ka of the upper Allier basin, because for this location and period the constraints of the available terrace dating techniques are tightest. The exercise will follow a stepwise approach of model parameterisation, calibration and validation in order to generate testable field predictions for future fieldwork.

Study Area

The study will focus on the Allier River system, a tributary of the Loire River, located in central France (see Figure 1(a)). The Allier river roughly flows from south to north, draining dominantly granitic massifs, with intermediate relief (below 1000 m) in the east (the Dore River tributary) and higher (up to 1880 m) (former) volcanic areas in the west (Cantal, Mont Dore, Chaîne de Puys feeding local tributaries). In the middle reach, mainly between Brioude and Vichy, a terrace record exists that has been extensively studied by us and other authors (Larue, 1979; Pastre, 1987, 2005; Veldkamp *et al.*, 2004). The Allier terraces are accurately mapped by the BRGM (2011) on basis of their morphology and relative position above the main river. The current floodplain is mapped as Fz; the first terrace up is mapped as the Holocene Fy terrace, followed by the MIS 2–4 Fx terrace. In some areas sublevels were mapped, subdividing the Weichselian Fx terrace into a higher Fxa (MIS 4) and a lower Fxb (MIS 2) terrace sublevel. The Fw terrace is correlated to MIS 12 to 6. Based on sand mineralogy, the Fw terrace was further subdivided into four sublevels (from old to young Fwa (MIS 12), Fwb (MIS 10), Fwc (MIS 8) and Fwd (MIS 6)) pushing back the time envelope to 400 ka (Pastre, 2005). Older terraces are mapped all the way up to the Pliocene (the Fs and Fl levels). Figure 1 shows the location, an example subdivision of the Fx terrace and a schematic Allier river terrace cross-section for the Limagne area near Clermont Ferrand (from Pastre, 2005). A more detailed lithostratigraphical subdivision for the Fx and Fwd terraces was made by Veldkamp and Kroonenberg (1993). They distinguished units based on sand bulk geochemical composition, reflecting differences in basaltic sand fraction (see Figure 1(b)). This subdivision in Fx-I, Fx-II, Fx-III and Fx-IV is also clearly visible in the field due to the different colours of the sedimentary units (see example photo Figure 2), where the boundary of Fx-I and Fx-III is remarkably clear with the basalt-rich Fx-III sublevel much more dark-greyish in colour than the underlying brownish basalt-poor Fx-I unit). The reconstructed lithostratigraphy demonstrates a complex stacking and nesting

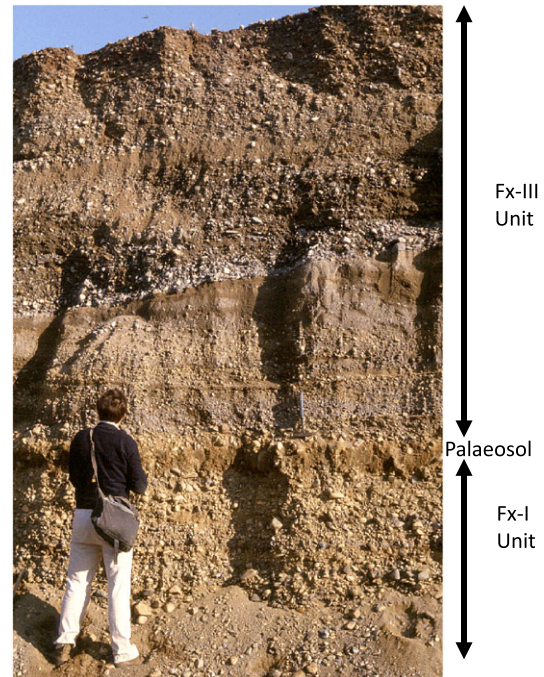


Figure 2. Example of a Fx terrace outcrop (located between Joze and Culhat). The photo illustrates two different litho-stratigraphic units in the field. The greyish basalt rich Fx-III is overlying the lower, basalt poorer Fx-I unit. Note palaeosol in between.

of different incision and aggradation phases within these Fx terraces, illustrating that the morphological subdivision of Fxa and Fxb as proposed by the BRGM (2011) is insufficient to capture the Late Quaternary fluvial dynamics in detail.

For the Allier terraces independent age estimates exist. The chronology of the older, long-term, Plio-Pleistocene record was established by correlating terrace sand mineralogy with the mineralogy of known K/Ar and Ar/Ar dated volcanic deposits (Pastre, 1987, 2005). His elaborate study demonstrated

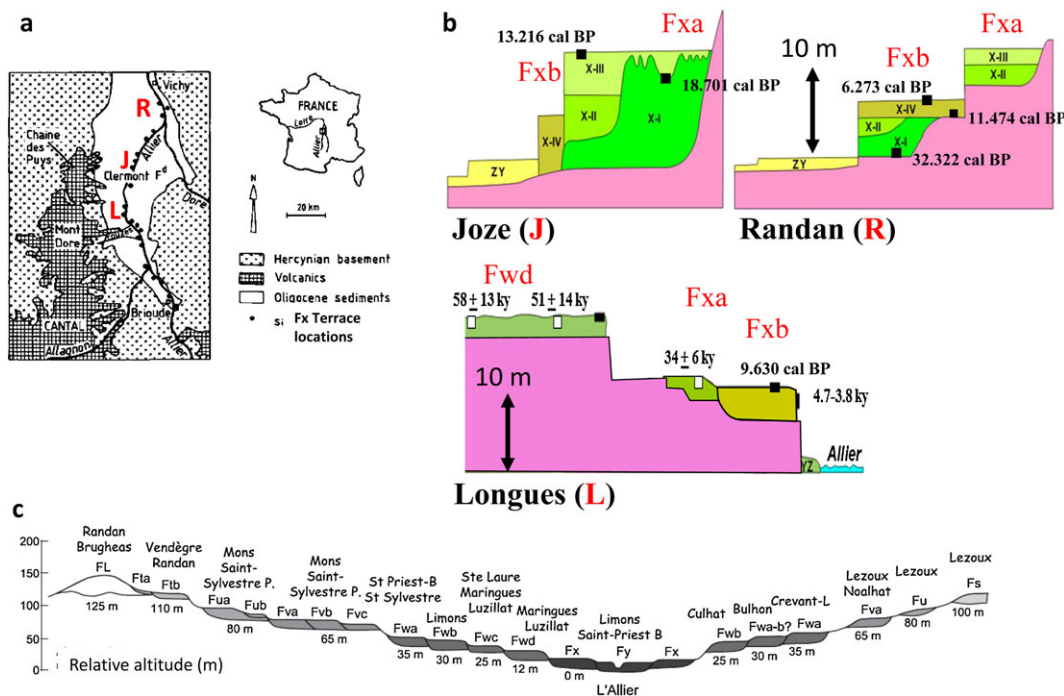


Figure 1. Terraces of the Allier river with (a) location map of the study area, (b) local Fx terrace stratigraphy near Longues, Joze and Randan (ages from Veldkamp and Kroonenberg, 1993; Rihs *et al.*, 2000; Veldkamp *et al.*, 2004), and (c) schematic Allier terrace staircase of study area (from Pastre, 2005).

the existence of a Plio-Pleistocene terrace staircase (see Figure 1(c)) with several distinct mineralogical markers of well dated Ar/Ar volcanic events. In total at least 25 different terrace units were distinguished spanning the last 3 Ma. For the last 1 Ma it appears that roughly every 100-ka, eccentricity-forced climate cycle generated at least one terrace unit (Veldkamp, 1992), but the age control is less certain as for the early Pleistocene terraces when the Mont Dore Massif was an active volcanic centre producing many large-scale and well-dated eruptions. This older volcanic history is best preserved in the well-dated volcano-sedimentary complex of the Perrier Plateau, where a palaeo-Allier valley and tributary with terraces are preserved below a complex of volcanic debris avalanche deposits (Pastre, 2004).

The methodology to correlate fluvial sand mineralogy with dated volcanic events is suitable for Plio-Pleistocene time-scales, but does not have sufficient temporal resolution to be applicable for the last 100 ka. Fortunately, the late Pleistocene record was dated directly using U-series and ^{14}C -radiometric methods at three different sites along the upstream Allier River. For the terraces near Longues, U-series dates of travertines capping the Fwb terrace indicate that terrace incision started at $58\text{--}51 \pm 14$ ka ago (Figure 1(b)). The sediments of the subsequently younger Fxa terrace were deposited afterwards and are capped by a 34 ± 6 ka old travertine, indicating an incisional phase around this time. The lower Fxb level stopped aggradation at 9.3 ka cal B.P. and was followed by a Holocene incision. Details of the samples and age estimates can be found in Rihs *et al.* (2000) and Veldkamp *et al.* (2004).

At Joze, two organic ^{14}C age estimates are available (Veldkamp and Kroonenberg, 1993). They indicate that the Fx-I terrace unit was deposited before 18.7 ka cal BP and that the deposition of Fx-III ceased at around 13.2 ka cal B.P. Together the ages indicate that the basalt-rich unit Fx-III was deposited between 18.7 and 13.2 ka ago. A ^{14}C -dated trachyandesitic tephra confirmed the pre 11.4 ka age of unit Fx-III (Juvigné *et al.*, 1992).

In the Randan region, there is a ^{14}C date of the base of the Fx-I unit of 32.3 ka cal B.P. For the Fx-IV/Fxb unit there are two ^{14}C ages. The base of a buried palaeosol gives a maximum age of 11.5 ka cal BP, while a buried palaeosol on top of the terrace gives a minimum age of 6.2 ka cal BP. Those two ages indicate a probable Younger Dryas age for the Fx-IV terrace unit (Veldkamp and Kroonenberg, 1993).

Landscape erosion rates

There are three independent erosion estimates available for the Allier basin. A study of the Lac Chambon infill and sediment budget during the last 13 ka (Macaire *et al.*, 1997) demonstrated a climate-dependent erosion rate ranging from $50\text{ m}^3/\text{km}^2/\text{yr}$ ($= 50\text{ mm}/\text{ka}$) during the Bölling interstadial to $120\text{ m}^3/\text{km}^2/\text{yr}$ ($= 120\text{ mm}/\text{ka}$) during the Younger Dryas stadial and returning again to $50\text{ m}^3/\text{km}^2/\text{yr}$ ($= 50\text{ mm}/\text{ka}$) during the prehistoric Holocene. These rates are certainly higher than the present average Allier basin rates because the Lac Chambon catchment was glaciated during the Late Weichselian with periglacial processes affecting the steep slopes and generating more sediments (Schaller *et al.*, 2002). Another independent estimate can be derived from calculated ^{10}Be erosion rates of fluvial quartz grains sampled from the terraces near the Allier-Dore confluence (Schaller *et al.*, 2002). Those estimated rates range from 40 mm/ka around 30 ka ago to a gradually increasing 70 mm/ka at the end of the Weichselian 10 ka ago, and then dropping to somewhat below 50 mm/ka during the late Holocene. These ^{10}Be erosion rates are considered to give systematic

overestimations due to the inherited ^{10}Be signal, which seems related to faster glacial erosion in its headwaters. That is why these authors also modelled glacial corrected erosion rates (Schaller *et al.*, 2002). The current river bed samples have an apparent age of around 15 ka indicating that they represent a 15 ka time-average erosion rate. The third independent erosion rate estimate is derived from 100-year river load gauge data of the Allier. These data yield much lower erosion rates, with an average of just below 10 mm/ka (see Schaller *et al.*, 2001, their Figure 3).

Because there is a terrace unit sequence with some independent age control of the last 50 ka and independent landscape erosion rate estimates for the same area, the study will focus modelling calibration and validation activities on the Fx terrace stratigraphy of that area and focus on the locations at Longues, Joze and Randan during this period. Longues is just downstream of the main tributaries draining the Mont Dore massif;

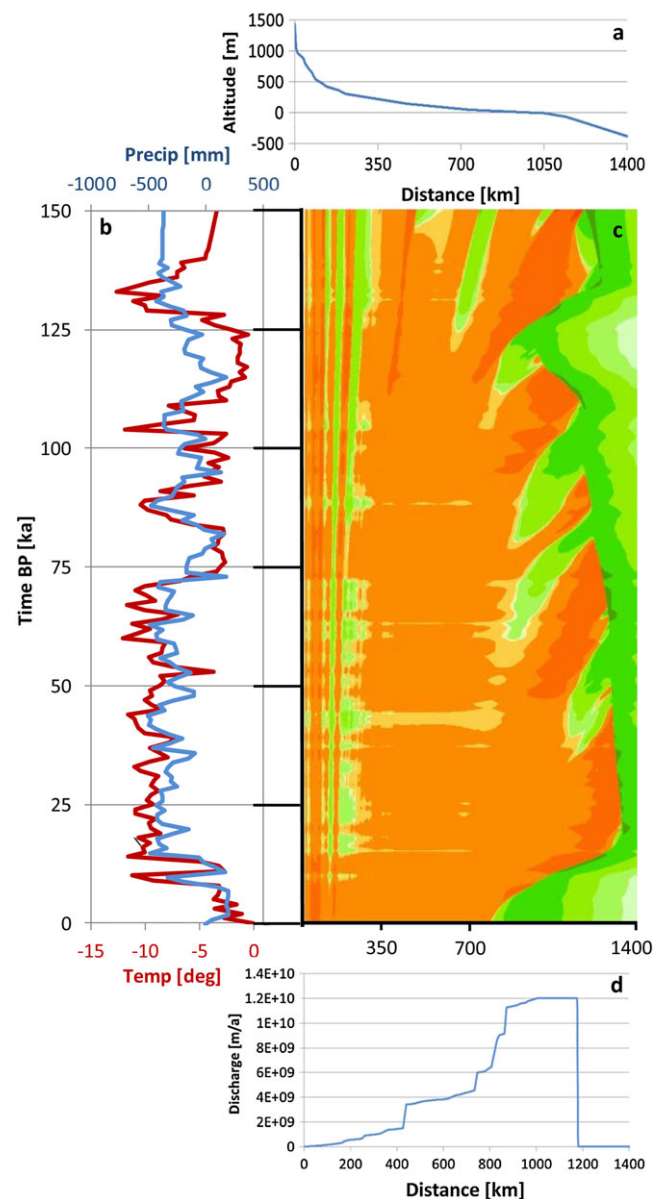


Figure 3. FLUVER2 Allier modelling exercise with relevant inputs and outputs with (a) input river gradient profile, (b) temperature (red) and precipitation (blue) deviations over the last 150 ka (Guiot *et al.*, 1989, 1993), (c) example of a Profile Evolution Map (PEM) with erosion (reds) and sedimentation (greens) along the 1400 km river profile and over the last 150 ka, and (d) discharge along the 1400 km river profile, note the drop in discharge around dynamic base-level.

Joze is downstream of the tributaries draining the Chaine des Puys and Randan is located just downstream of the Allier-Dore confluence (see Figure 1).

Methods

The FLUVER2 model structure was extensively described in previous publications (Veldkamp and van Dijke, 1998, 2000; Stemerink *et al.*, 2010), including sensitivity analysis (Tebbens and Veldkamp, 2001) and a systematic flowchart detailing the calculations by Geach *et al.* (2015) (their Figure 5). In this paper the model uses a forward modelling approach to simulate in time steps of 20 yr, the 1400-km (trunk length in increments of 1000 m) complete, Allier–Loire longitudinal profile including the shelf area, because this is part of the fluvial system during low stands. The model does not include marine currents during high stands that are crucial in lateral redistribution of the fluvial sediments, a known shortcoming of FLUVER2. The main equations used are given below (based on Veldkamp and Van Dijke, 1998, 2000). Symbols and units are given in Table I.

Sediment mass conservation:

$$\delta A / \delta t = -\delta L \delta x + U + Hill_sup \quad (1)$$

Sediment transport between river flow and substrate:

$$\delta F / \delta x = D - Tra_dis \quad (2)$$

Rate of sediment transfer from the river bed to the river flow:

$$D = K_fact G (\delta A / \delta x)^m \quad (3)$$

Rate of sediment transfer from the river flow to the river bed:

$$Tra_dis = L/h \quad (4)$$

Following the plea for clearer separation between field data used for model specification (input data and calibration; see Briant *et al.*, 2016) and that used for evaluation (validation data), we first describe the model inputs derived from field data followed by a section on the variables and related field data

Table I. Symbols including units and descriptions as used in Equations (1) to (4)

Symbol	Unit	Description
A	m	Altitude above reference level
T	s	Time
L	m ² s ⁻¹	Longitudinal sediment flux along the profile
X	m	Distance along longitudinal profile
U	m s ⁻¹	Uplift rate
Hill _{sup}	m s ⁻¹	Lateral influx rate of sediment from slopes
D	m s ⁻¹	Detachment rate from the substrate to sediment flow
Tra _{dis}	m s ⁻¹	Transfer rate from the sediment flow to the substrate
K _{fact}	m s ⁻¹	Erodibility of substrate
G	n. r.	Force function (discharge proxy), tuning variable
M	-	Erodibility exponent
H	m	Height difference

used for the model calibration. Lastly, the field data used for model validation and prediction are discussed.

Input data used for model specification

The main inputs are: 1) initial longitudinal profile; 2) uplift rate; 3) base-level change curve; and 4) two climate-related inputs, namely i) an effective precipitation curve and ii) hillslope-related sediment supply (see Figure 3).

Initial longitudinal profile

The shape of the initial longitudinal profile including the off-shore shelf (at 150 ka). We included the shelf because it becomes part of the longitudinal profile during low stands and it receives a lot of the upstream generated sediment. The profile was derived (at aggregated 1 km increments) from the current river profile (Figure 3(a)) which was extracted from the ASTER GDEM dataset (Reuter *et al.*, 2009; METI/NASA, 2015). This choice is based on the assumptions that i) the longitudinal profile has been in quasi-equilibrium during the late Quaternary, implying that river incision was able to keep pace with tectonic uplift and sediment supply (Bull, 1991) and ii) that no significant fault movements occurred separating the area in differently behaving tectonic units. Previous studies have shown that local tectonic block movements can significantly affect terrace formation and preservation (Viveen *et al.*, 2014).

Uplift rate

The classical way to estimate uplift rate is by reconstructing the valley incision rate using terrace altitude and age (Bridgland and Westaway, 2008). However, there are potentially significant uncertainties related to this methodology and there are indications that they can result in systematic overestimations when compared with other uplift rate estimates (Tebbens *et al.*, 2000; Hancock and Anderson, 2002; Schaller *et al.*, 2004).

We assume that the longitudinal river profile has been in quasi-equilibrium during the late Quaternary, implying that river incision was able to keep pace with tectonic uplift and sediment supply. This assumption implies that we can reconstruct the Allier incision rate (is assumed to be uplift rate) from the terrace staircase.

The work of Pastre (2005) and the review of Westaway (2004) both demonstrate that the current regime of uplift has been initiated during roughly the last million years. Using the relative terrace altitudes (measured from the current floodplain) and age correlations of Pastre (2005), and assuming an incisional-uplift equilibrium, an average uplift rate of 0.074 to 0.072 m/ka was calculated for the last 870–900 ka. This is the best average estimate possible. The Fva terrace is one of the few terraces that has been directly correlated with K/Ar dated volcanic eruptions (Coulées Pyro type Bozat). The related pumice layers can be traced in many Fva terrace exposures along the Allier (see Veldkamp 1992), allowing a chronostratigraphical marker to correlate current Fva terraces over >100 km, making this the only terrace that is not correlated on relative altitude and mineralogy only. The reconstructed uplift rate is slightly lower than the deducted uplift rate of 0.1 m/ka used by Veldkamp (1992), but it coincides well with the Late Quaternary rate proposed by Westaway (2004).

For modelling purposes a reconstructed constant uplift rate of 0.07 m/ka was used during the simulated timespan of 50 ka for the studied upper reach of the Allier River.

Base-level curve

The most up-to-date base-level (global sea level) curves are based on numerical modelling exercises of the waxing and waning of Northern Hemisphere ice sheets and changes in ocean surface temperatures (Bintanja *et al.*, 2005). Following the Viveen *et al.* (2013) FLUVER2 application, the modelled sea level time-series from Bintanja *et al.* (2005) was used with available time steps of 100 years as base-level input.

Climate-related inputs

Stemerding *et al.* (2010) demonstrated that sea surface temperature (SST) curves can yield a realistic proxy for precipitation in the North Atlantic coastal region of Europe. This approach was also successful for the Miño (Viveen *et al.*, 2013) and the Tabernas basins (Geach *et al.* 2015) using different ODP SST curves. For the Allier/Loire system this indirect methodology was not needed, as long and detailed pollen records (from the French lakes La Grande Pile, Les Bouchets and Les Echets) are available spanning the whole last Glacial/Interglacial cycle (Guiot *et al.*, 1989, 1993). The main pollen curves demonstrate a very good match and display clear changes from deciduous forest to open steppe and herbaceous tundra and then back to forest. From these pollen and related beetle records, both temperature and precipitation anomaly curves relative to present values were reconstructed for use as direct climate inputs (Guiot *et al.*, 1989, 1993). The precipitation curve was normalised to the present-day situation of annual effective precipitation, which translates into discharge (as the result of annual precipitation versus annual losses, e.g. evaporation, infiltration).

Consequently, there are two climate-related inputs, namely i) effective precipitation (function of the aforementioned annual precipitation anomalies) and ii) hillslope-related vegetation cover and sediment supply. These two inputs are independent and do show slightly different amplitudes and timings. They are used to calculate the discharge and sediment supply from tributaries in the basin by using the current DEM (contributing area and elevation potential, respectively). Figure 3(b) demonstrates the changes in average precipitation and temperature during the last 150 ka as used in the simulations (Guiot *et al.*, 1989, 1993). Discharge increase along the main river profile is calculated according to the total contributing area of all DEM-derived tributaries larger than 60 km² and divided over the 1000 m increments until the next tributary section comes in. In this way the total discharge follows a stepwise increasing pattern depending on catchment size (see Figure 3(d)).

The sediment supply from hillslopes is calculated as a function of the local relief potential in the contributing tributary catchments (highest potential found in the >1800 m.a.s.l. Mont Dore–Puy de Sancy area), normalised by the *Hill_sup* parameter and the temperature cooling and warming stages (temperature input, Guiot *et al.*, 1989, 1993). The rationale is that cooling results in ever less vegetation and more overland flow, which directly results in surface erosion, leading to a linear relationship between temperature and hillslope sediment supply. This approach deviates from that adopted by Stemerding *et al.* (2010) and Geach *et al.* (2015), who introduced discrete vegetation classes. The total amounts of sediments are then controlled by the tuning parameter *Hill_sup*, directly increasing or decreasing with the temperature amplitudes.

Model outputs

The model produces location- or reach-specific outputs for each time step as well as time slices for any variable projected along

the total length of the Allier river profile. Consequently, profile altitude, erosion – sedimentation dynamics or discharge can be produced at any time (see for example Figure 3(a) and (d)).

A very helpful graphic output is the Profile Evolution Map (PEM) which depicts erosion or sedimentation along the river profile on the horizontal axis over the simulation period on the vertical axis. The result is a map that shows the simulated dynamics along the river profile over space and time (see example in Figure 3(c)).

Final model calibration

The model is only calibrated on the basis of simple, general characteristics because over-calibration tends to remove the physical basis of a model (Mulligan and Wainwright, 2004, p. 55). During the calibration procedure the external input variables were first gradually included. The different steps and related model parameter setting are listed in Table 2 (Calfin 01 to Calfin 05). First base-level was added followed by uplift and subsequently precipitation and catchment erosion inputs combined with tributary water and sediment inputs. These inputs were not changed or used in the calibration as they are independently derived inputs (simply listed as switched 'on' in Table 2).

The more detailed calibration concerns the systematic exploring of the three internal parameters *Tra_dis* (sediment transport distance), *K_fact* (erodibility of material) and *Hill_sup* (sediment supply landscape) (see also Table 1 and Equations (1) to (4)).

They were incrementally adapted to obtain alternating erosion and depositional phases in the Allier river, since this behaviour is a minimum requirement for terrace formation. Subsequently, the focus was only on the last 50 ka for the Allier for the fine-tuning of the stepwise calibration.

First, for both internal parameters *Tra_dis* and *K_fact* their combined values were changed (Table 2 runs Calfin 06–13). Later, the *Hill_sup* parameter was changed (Table 2 runs Calfin 14–17). Finally, the *Tra_dis* and *Hill_sup* were both changed to obtain the best possible fits with the field data as detailed below (Table 2 runs Calfin 18–21).

Field-related data used in the calibration phase are: (A) the current geometry and altitude of the longitudinal profile. This approach is based on two assumptions: (i) the Allier longitudinal profile is in quasi-equilibrium (supported by the parallel terrace surfaces during the studied period); (ii) position and contributions of the Allier tributaries have not changed during the Late Quaternary. The model was always run for a longer timespan (150 ka) than the period of interest (50 ka) to remove artefacts caused by model disequilibrium during the start of the model run.

The other field data used for calibration concern (B) the observation that terraces occur along most of the longitudinal profile. This observation requires the model to produce alternating erosion and deposition cycles along its headwater reaches.

The final field data used are (C) average thickness of the terrace sedimentary bodies. This information is used to obtain realistic vertical aggradational space. This property is also indirectly related to terrace altitude but since terrace preservation is not simulated, terrace altitude was not used directly.

Model validation

Non-calibrated model outputs were used to compare them with known local terrace records as means of quasi-validation,

as suggested by Briant *et al.*, (2016). Independent field-derived data are used for model validity evaluation: (A) age of the terrace units, Fx-I to Fx-IV; (B) timing of aggradation and incision phases within these units for specific reaches; and (C) comparing reconstructed landscape erosion rates with the erosion rates required to generate the calibrated amount of hillslope sediment supply (*Hill_sup*).

Model prediction

The calibrated and quasi-validated FLUVER2 model version generated a record of reach specific fluvial dynamics along its longitudinal profile. For calibration purposes we used terrace location, altitude and thickness. Since the model does not mimic preservation, we cannot make predictions of current field occurrences. The only property not used in the calibration but for quasi-validation is the timing of erosion and deposition at specific locations. That leaves us with that property only to make some additional predictions. Ideally, when a model becomes available that can realistically simulate fluvial archive preservation we can predict where to expect which record preserved.

Results and Discussion

Calibration

All calibration steps are listed in Table II where each parameter setting is given. Figure 4 demonstrates the PEM output of Calfin 01 to 05, displaying the erosional and depositional changes along the longitudinal profile in time. It is obvious from the stepwise addition of more input variability (Figure 4(a): base run; Figure 4(b): inclusion of sealevel changes; Figure 4(c): inclusion of tectonic uplift; Figure 4(d): inclusion of climate-driven precipitation dynamics; Figure 4(e): inclusion of catchment erosion induced by vegetation dynamics) that the complexity of erosion and sedimentation patterns along the profile increases. Phases with a rise in base-level in the lowermost reaches of the Allier are associated with the upstream migration of a sedimentary

Table II. Parameter setting of calibration and sensitivity runs. Parameter units and descriptions as used in Equations (1) to (4) and in Table I. In italics the changed parameter values

Run	<i>Sealvl</i>	<i>Tect</i>	<i>Prec</i>	<i>Temp</i>	<i>Tra_dis</i>	<i>K_fact</i>	<i>Hill_sup</i>
Califin01	0	0	0	0	55000	1.11E-09	0
Califin02	<i>on</i>	0	0	0	55000	1.11E-09	0
Califin03	<i>on</i>	<i>0.00007</i>	0	0	55000	1.11E-09	0
Califin04	<i>on</i>	<i>0.00007</i>	<i>on</i>	0	55000	1.11E-09	0
Califin05	<i>on</i>	<i>0.00007</i>	<i>on</i>	<i>on</i>	55000	1.11E-09	<i>1.24E-08</i>
Califin06	<i>on</i>	<i>0.00007</i>	<i>on</i>	<i>on</i>	<i>65000</i>	1.11E-09	1.24E-08
Califin07	<i>on</i>	<i>0.00007</i>	<i>on</i>	<i>on</i>	<i>60000</i>	1.11E-09	1.24E-08
Califin08	<i>on</i>	<i>0.00007</i>	<i>on</i>	<i>on</i>	<i>50000</i>	1.11E-09	1.24E-08
Califin09	<i>on</i>	<i>0.00007</i>	<i>on</i>	<i>on</i>	<i>45000</i>	1.11E-09	1.24E-08
Califin10	<i>on</i>	<i>0.00007</i>	<i>on</i>	<i>on</i>	55000	<i>1.21E-09</i>	1.24E-08
Califin11	<i>on</i>	<i>0.00007</i>	<i>on</i>	<i>on</i>	55000	<i>1.16E-09</i>	1.24E-08
Califin12	<i>on</i>	<i>0.00007</i>	<i>on</i>	<i>on</i>	55000	<i>1.06E-09</i>	1.24E-08
Califin13	<i>on</i>	<i>0.00007</i>	<i>on</i>	<i>on</i>	55000	<i>1.01E-09</i>	1.24E-08
Califin14	<i>on</i>	<i>0.00007</i>	<i>on</i>	<i>on</i>	55000	1.11E-09	<i>3.24E-08</i>
Califin15	<i>on</i>	<i>0.00007</i>	<i>on</i>	<i>on</i>	55000	1.11E-09	<i>2.24E-08</i>
Califin16	<i>on</i>	<i>0.00007</i>	<i>on</i>	<i>on</i>	55000	1.11E-09	<i>6.35E-09</i>
Califin17	<i>on</i>	<i>0.00007</i>	<i>on</i>	<i>on</i>	55000	1.11E-09	<i>1.35E-09</i>
Califin18	<i>on</i>	<i>0.00007</i>	<i>on</i>	<i>on</i>	<i>60000</i>	<i>1.16E-09</i>	<i>4.24E-08</i>
Califin19	<i>on</i>	<i>0.00007</i>	<i>on</i>	<i>on</i>	<i>65000</i>	<i>1.11E-09</i>	<i>4.74E-08</i>
Califin20	<i>on</i>	<i>0.00007</i>	<i>on</i>	<i>on</i>	<i>60000</i>	<i>1.16E-09</i>	<i>4.74E-08</i>
Califin21	<i>on</i>	<i>0.00007</i>	<i>on</i>	<i>on</i>	<i>65000</i>	<i>1.21E-09</i>	<i>5.24E-08</i>

wedge. Deposition in the upstream reach of the Allier is linked to the cooler and drier phases of the Weichselian climate (Figure 4(e)). But overall erosional processes dominate, which is in tune with the uplift-driven incision of the Allier carving out a valley with terraces. The erosional/depositional dynamics of Calfin 05 are also plotted in Figure 3(c), where the link with the climate-related precipitation and catchment erosion inputs can be observed.

The apparent importance of base-level change in the lower reaches of the whole longitudinal profile could not be verified due to the lack of available data. It might explain the more complex architecture with many burial phases of the Loire terraces as described by Straffin *et al.* (1999). Unfortunately, the OSL dating done on those terraces is only reliable for the youngest terraces due to the high background radiation levels, as pointed out by Westaway (2004). The FLUVER2 simulations clearly indicate that base-level change had no direct effect on the upstream Allier reach where our study sites are located.

A subsequent stepwise calibration was run to investigate the effects of different *Tra_dis*, *K_fact* and *Hill_sup* values on the net vertical position of the river bed for the three reaches (Califin 06–21) using Calfin 05 as starting point. The changes for *Tra_dis* and *K_fact* have less impact on model outputs than *Hill_sup* (Figure 5(a) to (f)). Higher *Hill_sup* parameter values cause more aggradation while the erosion rates are higher too at all studied reaches (Figures 5(g) to (i)). We attempted to use higher values for *Hill_sup* but unfortunately this caused numerical model instability. The tendency towards numerical instability with high *Hill_sup* values was also observed and illustrated by stability plots (Tebbens and Veldkamp, 2001; Geach *et al.*, 2015, their Figure 6(A)). It illustrates a sensitive model balance between discharge-related erosion capacity (balanced by local gradients, *Tra_dis* and *K_fact*) and the sediment supply from tributaries (*Hill_sup*).

Figure 6 shows the PEMs for the last four calibration runs where all external driving factors are switched on and all three parameters have been fine-tuned to a maximum extent (Califin 18–21). In Table 2 the exact settings of *Tra_dis*, *K_fact* and *Hill_sup* can be found. Base-level change effects are only visible in the lowermost 700 km of the Allier, whereas in the uppermost 700 km of the headwaters alternating erosion and deposition phases occur that are related to erosion and sediment mobilisation from the surrounding catchments, which are in turn induced by cooling phases of the last glacial climate. This illustrates the relatively fast downstream migration of deposition zones and upstream migration of erosion zones in time. More pronounced is the alternation in time and the difference between the various simulations. Erosion and deposition dynamics are not occurring simultaneously along the whole longitudinal profile. Between simulations there are differences in rates when comparing specific locations, but overall it is difficult to appreciate the differences between the four PEMs in Figure 6.

A more specific calibration was therefore done on the vertical aggradation space at the three studied reaches near Longues, Joze and Randan. The net vertical development of the riverbed is illustrated in Figures 7(a), (b) and (c), whereas in Figures 7(c), (d) and (e) the vertical longitudinal changes (m/a) are shown, illustrating the vertical amplitude of local erosion/deposition dynamics at the different locations. The cumulative vertical aggradation during the last 50 ka is shown in Figures 7(g), (h) and (i).

The closest fit, considering the three calibration criteria, with the actual Allier Fx terrace properties was obtained with the Calfin 21 run (Figure 8). Therefore this version will be evaluated in more detail.

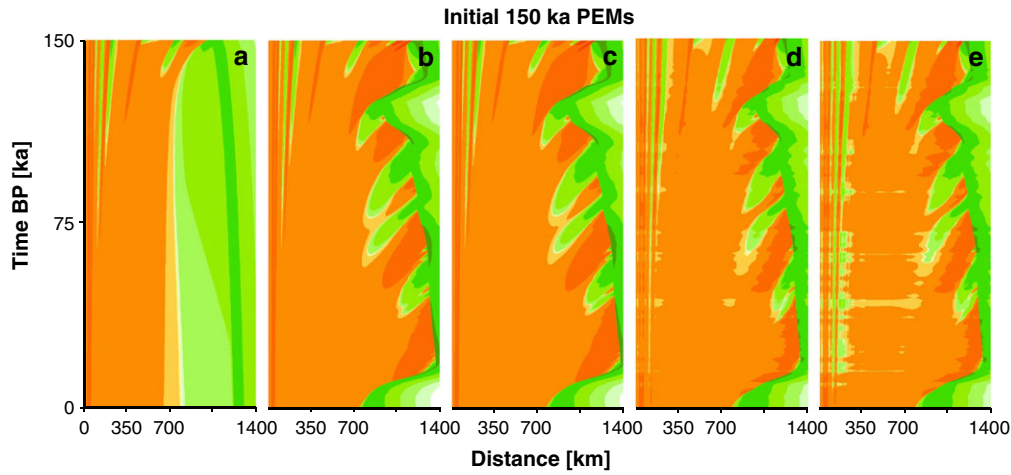


Figure 4. Initialising Allier PEMs over time (from 150 ka to present) of erosion (reds) and deposition (greens) along the river profile from the Allier headwaters (0 km) to continental shelf (1400 km) with increasing complexity: (a) base run Califin01; (b) Califin02 introducing sea-level fluctuations; (c) Califin03 adding tectonic uplift; (d) Califin04 adding climate-driven discharge; and (e) Califin05 adding climate-driven hillslope sediment input. See Table II for parameter settings.

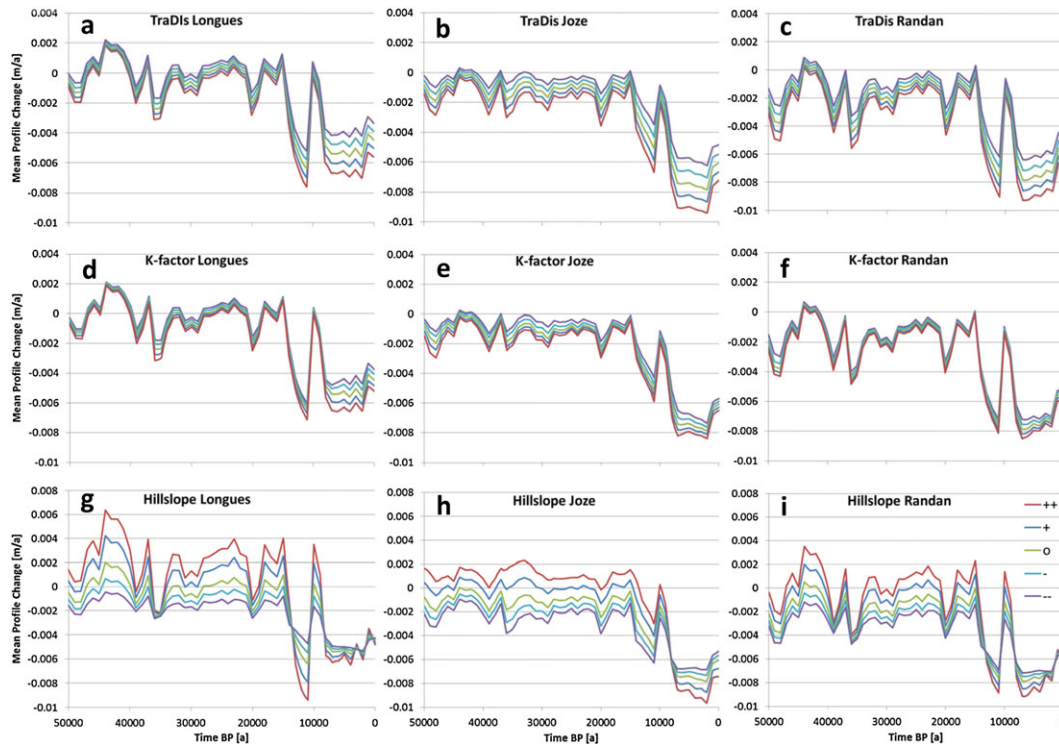


Figure 5. Sensitivity simulations over the last 50 ka of erosion–sedimentation dynamics for parameter change (decreasing -, – – and increasing +, ++ at three locations for sediment travel distance (Califin06–Califin09) *Tra_dis* (a, b, c), (Califin10–Califin13) *K_fact* (d, e, f) and (Califin14–Califin17) *Hill_sup* (g, h, i). Note different Y-axis scaling for the 3 *Tra_dis*, *K_factor* and *Hill_sup* locations. The parameter settings of the different runs (Califin) are listed in Table II.

Model output evaluation

Figure 8 is focused on the Allier part of the simulated system for the last 50 ka for two reasons: (1) only the Allier at Longues, Joze and Randan reaches were calibrated; and (2) only independent field data is available for those reaches. In Figure 8(a) the upper longitudinal profile is plotted showing the Allier and the Loire downstream of their confluence. This confluence stands out in Figure 8(b), where the discharge is plotted along the longitudinal profile as the largest increase in discharge. The three reaches at Longues, Joze and Randan (locations are indicated in Figure 8(c)) all have tributaries in between them and demonstrate in the PEM significant amounts of sub-

synchronous change of erosion and deposition phases. There is only a delayed response of a few hundred to thousand years maximum (Figure 8(c)). The erosion/deposition patterns change along the longitudinal profile when a major tributary joins the Allier. The PEM shows some tributary-related compartmentation. This indicates that the reach-specific sediment supply dynamics are related to the tributaries (see Figure 1 locations of Couzes draining the Mont Dore massif and Dore river). The observed differences are linked to size and relief of the tributary basins. Overall there is a match (accepting an uncertainty of ± 2 ka) of the main aggradation phases at 45–40 ka, 30–20 ka, 18–12 ka and around 10 ka BP for the whole upper 700 km profile (table in Figure 9 and ages in Figure 1). Incisional phases

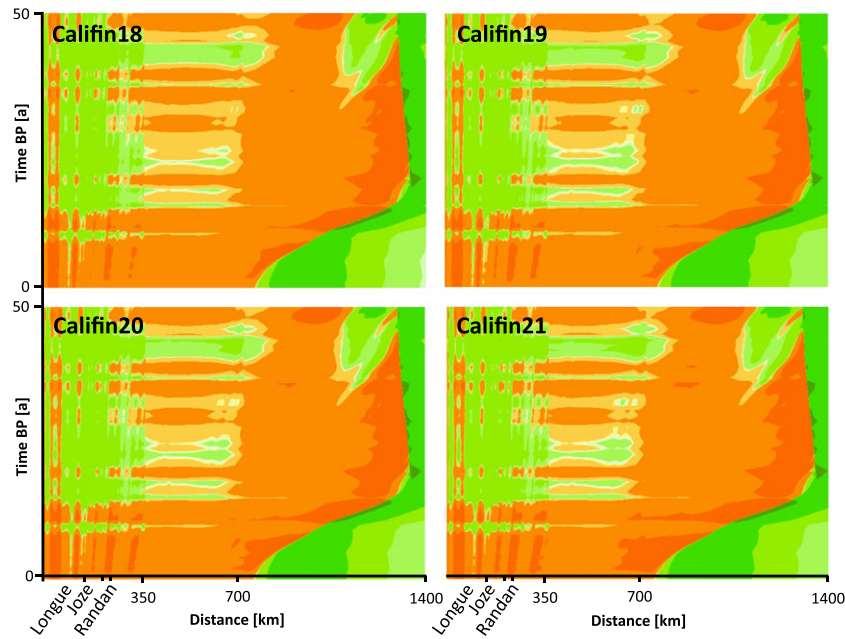


Figure 6. PEMs of 50 ka simulations for Califin runs 18, 19, 20 and 21 (see Table II) where all three parameters were modified in order to get the 'best' fit. Locations of Longue, Joze and Randan along the river profile indicated below (see also Figure 1).

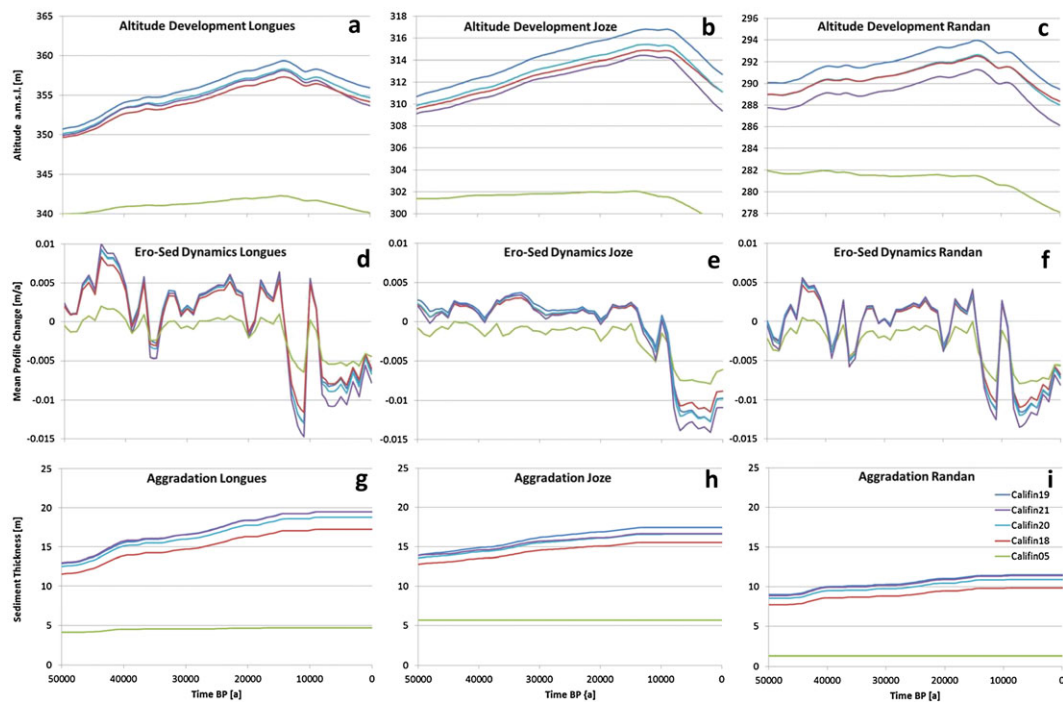


Figure 7. Simulation outputs locations Longue, Joze, Randan Califin18–21 for 50 ka (i) altitude development a.m.s.l. (a, b, c), (ii) erosion (negative) and sedimentation dynamics (d, e, f), and (iii) potential terrace thickness (g, h, i) for locations near Longues (a, d, g), Joze (b, e, h) and Randan (c, f, i). Note different Y-axis scaling for a, b and c.

are modelled around 50–45 ka, 40–30 ka, 20 ka, 12–11 ka and 10–0 ka B.P., and often coincide with the warmer and wetter periods (Figure 8(c) and (d) and table in Figure 9).

Validation

Overall the known age chronology of the Allier (see Figure 1) and the Loire near the Allier/Loire confluence (Straffin *et al.*, 1999) seem to confirm the overall dynamics as described above (Figure 8). But such a general observation is not considered suitable as a validation.

There are also clear differences in the simulated, temporal, vertical erosion and sedimentation dynamics for the three locations, a property which was not used during model calibration (Figure 9). Not only is the timing slightly different, also the vertical dynamics are different at the three locations. For example at Longues several erosional phases occur at 38, 34 and 19 ka which are almost absent at Joze, while no fewer than five erosional phases occur downstream near Randan during the same time span. This difference is most obvious for the incisional phase that can be tentatively linked to the late glacial warming event, followed by the Younger Dryas aggradation event at 10 ¹⁴C ka. Both are very pronounced at Longues and

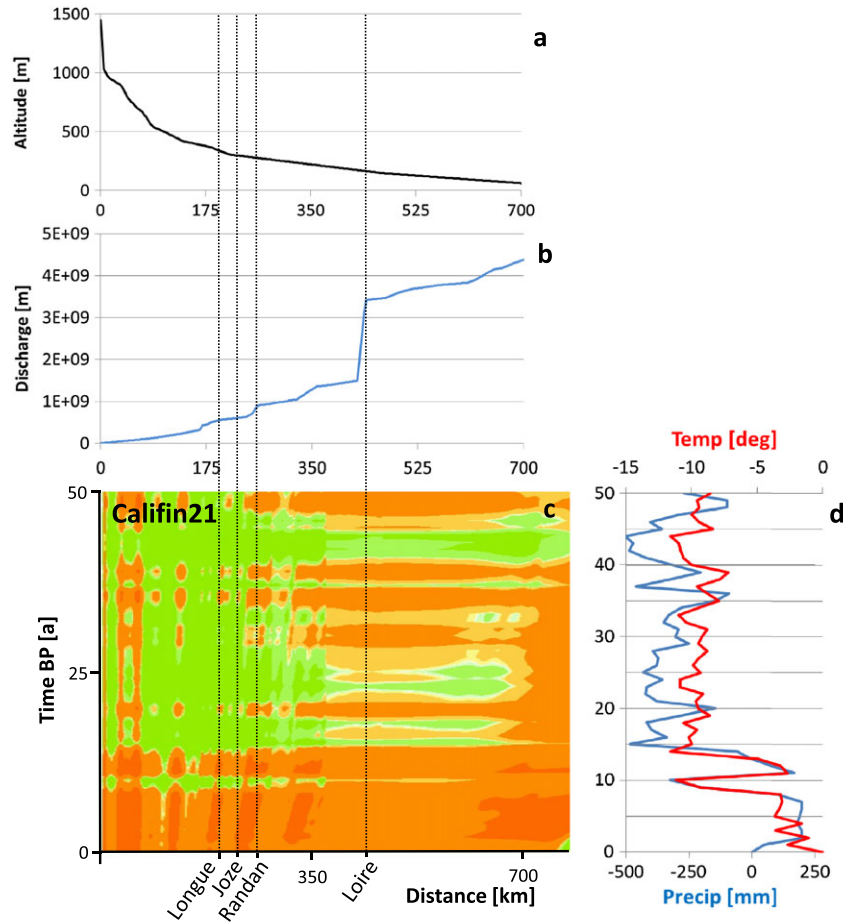
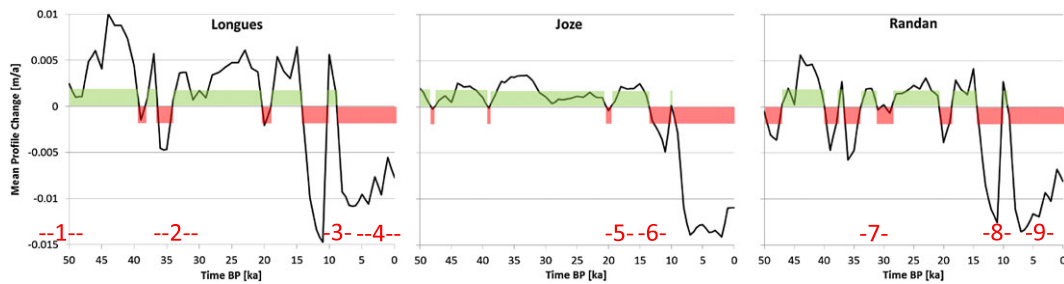


Figure 8. Details of simulation of Califin run 21, only the first 700 km detail of a 50 ka PEM, with (a) Allier river gradient length profile, (b) example accumulative discharge (at $t = 50$ ka), (c) PEM of erosion (reds) and sedimentation (greens), and (d) climate inputs: temperature (red) and precipitation (blue) anomalies (Guiot *et al.*, 1989, 1993). Locations of Longue, Joze and Randan (see also Figure 3), and the confluence with the Loire are indicated below (c).



Location	Original age BP	Cal age BP	Organic matter
1: Longues Wb	58.000 ± 13.000	n.a.	Travertine cap U/Th related to water table lowering due to incision of terrace
2: Longues Xa	34.000 ± 6.000	n.a.	Travertine cap U/Th related to water table lowering due to incision of terrace
3: Longues Xb	9.630 ± 90	9.260	Stability phase before incision Fxb
4: Longues Xb scarp	4.700 and 3800	n.a.	Travertine in the terrace scarp is post incision, 4.7 ky (by means of 226Ra decrease) and 3.8 ky (by means of 26Ra/Ba) (sample TA 6 in Rihs <i>et al.</i> , 2000)
5: Joze top X-III	12.370 ± 200	13.216	during end of aggradation Fx-III and lake phase Marais.
6: Joze top X-I	16.585 ± 250	18.701	Stability phase after aggradation Fx-I in gully and before aggradation Fx-III
7: Randan base X-I	29.560 ± 300	32.322	Stability phase in gully before main aggradation Fx-I
8: Randan base X-IV	11.380 ± 100	11.474	Stability phase (burried palaeosol) before aggradation Fx-IV
9: Randan top X-IV	7.310 ± 70	6.273	Stability phase (burried palaeosol) after incision Fx-IV

Figure 9. The Califin21 run displaying the vertical erosional and depositional dynamics at Longues, Joze and Randan. The numbers indicate existing ages based on U-series of ^{14}C dating. Calibration of ^{14}C ages was done with OxCal. Inset table explains sample locations and settings.

Randan and much more subdued at Joze. This might explain why the Fx terrace at both Longues and Randan have a Fxa late glacial sublevel and a presumably Younger Dryas Fxb sublevel, while this is hardly the case near Joze (Figure 1(b) and see BRGM (2011) 1:50.000 geology maps).

The vertical amplitude of both erosion and deposition phases is much more pronounced at Longues and Randan when compared to Joze (Figure 9). It demonstrates the higher potential for the formation of two separate terraces (Fxa and Fxb) at Longues and Randan compared to the Joze section. Also, the maximum

aggradation thickness (Figure 6(g) to (i)) declines from 8 m near Longues to 5 m downstream near Randan. This is an underestimation compared to field values ranging from 5 to 12 m.

The vertical erosion and depositional dynamics were plotted together with the available age estimates in Figure 9. Each age estimate represents a different condition. For the Longues section most travertine dates coincide with the initiation of an incisional phase, while the ^{14}C dates at Joze and Randan are often from organic remains associated with either a vegetation phase in a gully or a buried palaeosol. There is a good match for all three locations, despite the age uncertainties, between the detailed vertical dynamics as generated by the model and the existing age control. Model outputs for the last 11 ka seem to indicate a close relationship with known climate fluctuations.

The third independent option for a validation is the comparison between the modelled and calibrated erosion rates from the surrounding catchments, and the independently measured landscape erosion rates. Figure 10 gives the maximum and minimum simulated hillslope erosion in the Allier valley near the Allier/Dore confluence and the erosion rates that were discussed earlier in this paper (from Schaller *et al.*, 2002). The minimum–maximum curves give a range of 1 ka averaged landscape erosion rates that are required to generate the sediment flux inputs that were tuned during the calibration phase. The ^{10}Be rates (15 ka averages) are plotted as generated by Schaller *et al.* (2002) and include both the measured and glaciation-corrected (to correct for glacial erosion overestimation) values. With a perfect match one would expect the ^{10}Be erosion rates to plot between the maximum and minimum rates, with an exception for the Holocene where the 15 ka average erosion rate will smooth out the high Late Glacial and low Holocene rates, causing an overestimation for the Holocene erosion rates (Schaller *et al.*, 2001). The maximum simulated *Hill_{sup}* erosion rates are generally close to measured rates, suggesting a systematic underestimation of erosion rates, assuming the ^{10}Be data are realistic values. The expected deviation for the Holocene occurs but for this time span the modelled rates fit well with the 100 yr river sediment gauge data (* in Figure 10) (Schaller *et al.*, 2001), while the model uses 20 yr average rates.

Figure 10 indicates that the calibration resulted in erosion rates of the same order of magnitude as measured, and that the erosion rate values show similar trends of increase and decrease in time. On average the simulated erosion rate appears to be somewhat lower than measured. Combined with the

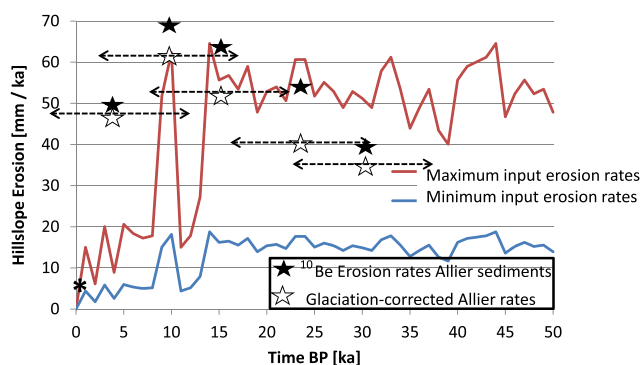


Figure 10. Minimum (blue line) and maximum (red line) hillslope input erosion rates for simulation Califin21 over the last 50 ka. Minimum rates represent the areas in the east, mainly the Dore river catchment and maximum rates in the west from the Allier (tributaries) draining the Mont Dore and Cantal volcanic higher areas. Black and white stars indicate ^{10}Be erosion rates from Schaller *et al.* (2002) which are 15 ka averages (temporal range indicated with arrows). The * indicates the 100 years river bedload gauge data erosion rate from (Schaller *et al.*, 2001).

observation that the 5 to 8 m sediment aggradation in the model is less than the observed 5 to 12 m, a somewhat higher simulated hillslope sediment supply rate (and related landscape erosion rate) appears to be desirable for a perfect calibration. Unfortunately this was not possible due to the previously mentioned numerical instability problems, which appear to be indicative of oversaturation of the system with sediments. This points to a fundamental limitation of FLUVER2, namely the lack of a horizontal dimension for channel widening to allow channel avulsions and increasing sediment accommodation space.

In general the model output displays significant reach-specific differences (Figure 9) which at first sight – given known age uncertainties – are explained by the existing field data (Figures 1 and 10). It was already noted from the match of Figure 8(b) and 8(c) that each time a major tributary joins the Allier, the local erosion/deposition dynamics pattern changes. This effect declines downstream near the Allier/Loire confluence (marked Loire in Figure 8). Apparently this reach-specificity is occurring more in the headwaters where there are more important tributaries compared to the trunk system. The apparent uniformity of the erosional and depositional dynamics along the longitudinal profile near the Allier/Loire confluence could be an interesting testable hypothesis for future field work. The model confirms the observed complexity of the three studied reaches along the Allier. It also suggests strongly that using only terrace morphological units is insufficient to reconstruct the more complex dynamics in time.

Overall can it be observed that a relatively simple model such as FLUVER2, using known straightforward external drivers, produces intriguing reach-specific dynamics that are supported by existing field evidence not used in the calibration. It suggests that the model mimics past dynamics sufficiently realistically to guide future field work.

Making specific testable field predictions

Since no location-specific aggradation and erosion timing were taken into account during the calibration of FLUVER2, these properties can be used to make quasi-independent predictions from the model version. This implies that for some non-dated terrace units independent age predictions can be made based on the model runs. It can be observed that the timing of aggradation and incision events is not similar for the three locations. For example the 41 and 35 ka incisional phases at Longues and Randan are almost absent at Joze. This implies that there appears to be an almost continuous (no major erosional phase) build-up between 50 and 15 ka BP of the Joze terrace body.

There are only a few published age estimates for the older units within the Fx terraces, even though the medium-to-coarse sandy units are in principal suitable for OSL dating of quartz or feldspar grains. OSL dating has not been done yet for the three reaches and would, if successful, certainly add new insights. The temporal delays of some depositional or erosional events between the three reaches are unfortunately close to the typical uncertainty range of the currently available OSL dating techniques. Taking these uncertainties into account, it can be predicted that systematic OSL sampling of the Fx terraces outcrops near Joze will yield ages that gradually decrease from bottom to top from 50 to 12 ka old. On the other hand will the terrace sediment ages at Longues and Randan demonstrate more hiatuses in their age distribution. The aggradation units in Figure 9 give a clear prediction which ages to expect at the three different locations.

Additional predictions are aimed at dating easily recognisable settings such as the transition of Fx-II to Fx-III at

Joze and Randan. The model outcomes predict this contact will be 20 ka old and that at Joze there will be a smaller temporal hiatus than at Randan where more erosion took place between the two aggradation events. More detailed predictions are not realistic given the uncertainties associated with current dating methodologies (Stokes *et al.*, 2012).

Conclusions

A calibrated and quasi-validated FLUVER2 model version for the Allier suggests that there is strong reach dependency in the registration of past fluvial dynamics. A first comparison with independent, available field data not only confirms this characteristic but also demonstrates a good match with known timing of erosion or depositional phases.

Concrete, testable predictions are proposed of the timing and location of aggradation and erosion phases at the three studied locations.

It is the intention to organise field work to attempt checking these predictions with OSL dating to test the reach-specific dynamics and timing produced by the best calibrated model version. When this is done, it will be the first time that a numerical modelling exercise guides fieldwork and sampling. Only if the predicted properties are confirmed, it will demonstrate that model simulations have some ability to predict detailed fluvial records by identifying where and when specific climatic periods are registered in the fluvial record.

Acknowledgments—This paper was initiated during the fruitful FAC-SIMILE workshops at the faculty ITC, University Twente in December 2013 and 2014. J. Guiot is kindly thanked for providing the raw climate data.

References

- Baartman JEM, Temme AJAM, Veldkamp T, Jetten VG, Schoorl JM. 2013. Exploring the role of rainfall variability and extreme events in long-term landscape development. *Catena* **109**: 25–38.
- Bintanja R, Van de Wal RSW, Oerlemans J. 2005. Modelled atmospheric temperatures and global sea levels over the past million years. *Nature* **437**: 125–128.
- Blum MD, Törnqvist TE. 2000. Fluvial responses to climate and sea-level change: a review and look forward. *Sedimentology* **47**: 2–48.
- BRGM. 2011. Bureau de Recherches Géologiques et Minières 1:50 000 geological maps of France. More detailed information available at <http://www.brgm.eu/activities/geology/geological-map-of-france>.
- Briant RM, Cohen KM, Cordier S, Demoulin A, Macklin MG, Mather A, Rixhon G, Veldkamp A, Wainwright J, Whittaker A, Wittmann H. 2016. State of science: does current fieldwork practice enable effective field-model comparison of fluvial landscape evolution? *Earth Surface Processes and Landforms* (Unpublished).
- Bridgland D, Westaway R. 2008. Climatically controlled river terrace staircases: A worldwide Quaternary phenomenon. *Geomorphology* **98**(3–4): 285–315.
- Bull WB. 1991. *Geomorphic Responses to Climatic Change*. Oxford University Press: New York.
- Cordier S, Frechen M, Harmand D. 2014. Dating fluvial erosion: fluvial response to climate change in the Moselle catchment (France, Germany) since the Late Saalian. *Boreas* **43**: 450–468.
- Coulthard TJ, Van de Wiel MJ. 2013. Climate, tectonics or morphology: what signals can we see in drainage basin sediment yields? *Earth Surface Dynamics* **1**: 67–91.
- Coulthard TJ, Macklin MG, Kirkby MJ. 2002. Simulating upland river catchment and alluvial fan evolution. *Earth Surface Processes and Landforms* **27**: 269–288.
- Forzoni A, Storms JE, Whittaker AC, de Jager G. 2014. Delayed delivery from the sediment factory: modeling the impact of catchment response time to tectonics on sediment flux and fluvio-deltaic stratigraphy. *Earth Surface Processes and Landforms* **39**(5): 689–704.
- Gargani J, Stab O, Cojan I, Brulhet J. 2006. Modelling the long-term fluvial erosion of the River Somme during the last million years. *Terra Nova* **18**(2): 118–129.
- Gasparini NM, Bras R, Whipple KX. 2006. Numerical modeling of non-steady-state river profile evolution using a sediment-flux-dependent incision model. *Special paper of the Geological Society of America* **398**: 127–141.
- Geach MR, Viveen W, Mather AE, Telfer MW, Fletcher WJ, Stokes M, Peyron O. 2015. An integrated field and numerical modelling study of controls on Late Quaternary fluvial landscape development (Tabernas, southeast Spain). *Earth Surface Processes and Landforms* **40**: 1907–1926. DOI:10.1002/esp.3768.
- Guiot J, Pons A, De Beaulieu JL, Reille M. 1989. A 140,000-year continental climate reconstruction from two European pollen records. *Nature* **338**(6213): 309–313.
- Guiot J, de Beaulieu JL, Cheddadi R, David F, Ponel P, Reille M. 1993. The climate in Western Europe during the last Glacial/Interglacial cycle derived from pollen and insect remains. *Palaeogeography, Palaeoclimatology, Palaeoecology* **103**(1–2): 73–93.
- Hancock GS, Anderson RS. 2002. Numerical modeling of fluvial strath-terrace formation in response to oscillating climate. *Geological Society of America Bulletin* **114**(9): 1131–1142. DOI:10.1130/0016-7606.
- Juvigné EH, Kroonenberg SB, Veldkamp A, El Arabi A, Vernet G. 1992. Widespread Alleröd and boreal trachyandesitic to trachytic tephra layers as stratigraphical markers in the Massif Central, France. *Quaternaire* **3**: 137–146.
- Larue JP. 1979. Les nappes alluviales de la Loire et de ses affluents dans le Massif Central et dans le Sud du Bassin parisien. Étude géomorphologique. Thèse de doctorat ès Lettres, Clermont-Ferrand.
- Macaire J-J, Bossuet G, Choquier A, Cocirta C, De Luca P, Dupis A, Gay I, Mathey E, Guenet P. 1997. Sediment yield during Late Glacial and Holocene periods in the Lac Chambon watershed, Massif Central, France. *Earth Surface Processes and Landforms* **22**: 473–489.
- Maddy D, Demir T, Veldkamp A, Bridgland DR, Stemerink C, van der Schriek T, Schreve D. 2012. The obliquity-controlled early Pleistocene terrace sequence of the Gediz River, western Turkey: a revised correlation and chronology. *Journal of the Geological Society* **169**: 67–82. DOI:10.1144/0016-76492011-011.
- METI/NASA, 2015. ASTER Global Digital Elevation Model. Ministry of Economy, Trade and Industry of Japan (METI) and the National Aeronautics and Space Administration (NASA). <http://asterweb.jpl.nasa.gov/gdem.asp> and <http://www.gdem.aster.ersdac.or.jp/> accessed February 2015.
- Mulligan M, Wainwright J. 2004. Modelling and model building. In *Environmental Modelling: Finding Simplicity in Complexity*, Mulligan M, Wainwright J (eds). Wiley: Chichester; 7–73.
- Oreskes N, Shrader-Frechette K, Belitz K. 1994. Verification, validation, and confirmation of numerical models in the earth sciences. *Science* **263**: 641–646.
- Pastre J-F. 1987. Les formations plio-quaternaires du bassin de l'Allier et le volcanisme régional (Massif Central, France). Rapports géodynamiques, corrélations téphrochronologiques, implications. Thèse de doctorat de l'Université Paris VI – Mémoires des Sciences de la Terre Université Curie, Paris no 87–32.
- Pastre J-F. 2004. The Perrier Plateau: a Plio-Pleistocene long fluvial record in the river Allier Basin, Massif Central, France. *Quaternaire* **15**(1): 87–101.
- Pastre J-F. 2005. Les nappes alluviales de l'Allier en Limagne (Massif Central, France): stratigraphie et corrélations avec le volcanisme régional. (The river Allier terraces in Limagne (France): Stratigraphy and correlation with the Massif Central volcanism). *Quaternaire* **16**: 153–175.
- Reuter HI, Nelson A, Strobl P, Mehl W, Jarvis A, 2009. A first assessment of aster GDEM tiles for absolute accuracy, relative accuracy and terrain parameters. In *International Geoscience and Remote Sensing Symposium (IGARSS)* **5**, 5417688, V240–V243.
- Rihs S, Condomines M, Poidevin J-L. 2000. Long-term behaviour of continental hydrothermal systems: U-series study of hydrothermal carbonates from the French Massif Central (Allier valley). *Geochimica et Cosmochimica Acta* **64**: 3189–3199.

- Sapozhnikov VB, Murray AB, Paola C, Foufoula-Georgiou E. 1998. Validation of braided-stream models: spatial state-space plots, self-affine scaling and island shapes. *Water Resources Research* **34**(9): 2353–2364.
- Schaller M, von Blanckenburg F, Hovius N, Kubik PW. 2001. Large-scale erosion rates from in situ-produced cosmogenic nuclides in European river sediments. *Earth and Planetary Science Letters* **188**: 441–458.
- Schaller M, von Blanckenburg F, Veldkamp A, Tebbens LA, Hovius N, Kubik PW. 2002. A 30 000 yr record of erosion rates from cosmogenic ¹⁰Be in Middle European river terraces. *Earth and Planetary Science Letters* **204**: 307–320.
- Schaller M, von Blanckenburg F, Hovius N, Veldkamp A, van den Berg MW, Kubik PW. 2004. Paleocorrosion rates from cosmogenic ¹⁰Be in a 1.3 Ma terrace sequence: Response of the river Meuse to changes in climate and rock uplift. *Journal of Geology* **112**(2): 127–144.
- Schoorl JM, Veldkamp A. 2003. Late Cenozoic landscape development and its tectonic implications for the Guadalhorce valley (South Spain). *Geomorphology* **50**(1–3): 43–57.
- Schoorl JM, Temme AJAM, Veldkamp A. 2014. Modelling centennial sediment waves in an eroding landscape – catchment complexity. *Earth Surface Processes and Landforms* **39**: 1526–1537. DOI:10.1002/esp.3605.
- Schumm SA. 1977. *The Fluvial System*. Wiley: New York.
- Schumm SA. 1993. River response to baselevel change: implications for sequence stratigraphy. *Journal of Geology* **101**: 279–294.
- Stange KM, Van Balen RT, Garcia-Castellanos D, Cloetingh S. 2016. Numerical modelling of Quaternary terrace staircase formation in the Ebro foreland basin, southern Pyrenees, NE Iberia. *Basin Research* **28**: 124–146. DOI:10.1111/bre.12103.
- Stemerink C, Maddy D, Bridgland DR, Veldkamp A. 2010. The construction of a palaeodischarge time series for use in a study of fluvial system development of the middle to late pleistocene upper Thames. *Journal of Quaternary Science* **25**(4): 447–460.
- Stokes M, Cunha PP, Martins AA. 2012. Techniques for analysing Late Cenozoic river terrace sequences (Editorial). *Geomorphology* **165–166**: 1–6.
- Straffin E, Blum M, Colls A, Stoker S. 1999. Alluvial stratigraphy of the Loire and Arroux rivers (Burgundy, France). *Quaternaire* **10**: 271–282.
- Tebbens LA, Veldkamp A. 2000. Late Quaternary evolution of fluvial sediment composition: a modeling case study of the River Meuse. *Global and Planetary Change* **27**: 187–206.
- Tebbens LA, Veldkamp A. 2001. Exploring the possibilities and limitations of modelling Quaternary fluvial dynamics: a case study of the river Meuse. In *River Basin Sediment Systems: Archives of Environmental Change*, Maddy D, Macklin MG, Woodward JC (eds). Balkema: Rotterdam, 2001. - ISBN 90 5809 342 5 - 469–484.
- Tebbens LA, Veldkamp A, van Dijke JJ, Schoorl JM. 2000. Modeling longitudinal-profile development in response to Late Quaternary tectonics, climate and sea-level changes: the River Meuse. *Global and Planetary Change* **27**: 165–186.
- Temme AJAM, Armitage J, Attal M, van Gorp W, Coulthard T, Schoorl JM. 2016. Choosing and using landscape evolution models to inform field-stratigraphy and landscape reconstruction studies. *Earth Surface Processes and Landforms* (in review for this issue) EDITOR: Latest info required.
- Temme AJAM, Claessens L, Veldkamp A, Schoorl JM. 2011. Evaluating choices in multi-process landscape evolution models. *Geomorphology* **125**: 271–281.
- Tucker GE, Hancock GR. 2010. Modelling landscape evolution. *Earth Surface Processes and Landforms* **35**: 28–50. DOI:10.1002/esp.1952.
- Van Balen RT, Busschers FSA, Tucker GE. 2010. Modeling the response of the Rhine-Meuse fluvial system to Late Pleistocene climate change. *Geomorphology* **114**: 440–452.
- Van Gorp W, Temme AJAM, Veldkamp A, Schoorl JM. 2015. Modelling long-term (300 ka) upland catchment response to multiple lava damming events. *Earth Surface Processes and Landforms* **40**(7): 888–900.
- Veldkamp A. 1992. A 3-D model of fluvial terrace development in the Allier basin (Limagne, France). *Earth Surface Processes and Landforms* **17**: 487–500.
- Veldkamp A, Kroonenberg SB. 1993. Late Quaternary chronology of the Allier terrace sediments (Massif Central, France). *Geologie en Mijnbouw* **72**: 179–192.
- Veldkamp A, Tebbens LA. 2001. Registration of abrupt climate changes within fluvial systems: insights from numerical modelling experiments. *Global and Planetary Change* **28**: 129–144.
- Veldkamp A, van Dijke JJ. 1998. Modelling long-term erosion and sedimentation processes in fluvial systems: a case study for the Allier, Loire system. In *Palaeohydrology and Environmental Change*, Benito G, Baker VR, Gregory KJ (eds). Wiley: Chichester; 53–66.
- Veldkamp A, van Dijke JJ. 2000. Simulating internal and external controls on fluvial terrace stratigraphy: a qualitative comparison with the Maas record. *Geomorphology* **33**: 225–236.
- Veldkamp A, Van den Berg MW, Van ijke JJ, de Berg van Saparoea RM. 2002. Reconstructing Late Quaternary fluvial process controls in the upper Aller Valley (North Germany) by means of numerical modelling. *Geologie en Mijnbouw* **81**: 375–388.
- Veldkamp A, Kroonenberg SB, Heijnis H, van den Berg van Saparoea R. 2004. The suitability of dated travertines as a record of fluvial incision: Allier (France) floodplain dynamics during the late Quaternary. *Quaternaire* **15**: 159–165.
- Viveen W, Schoorl JM, Veldkamp A, van Balen RT, Desprat S, Vidal-Romani JR. 2013. Reconstructing the interacting effects of base level, climate, and tectonic uplift in the lower Miño River terrace record: a gradient modelling evaluation. *Geomorphology* **186**: 96–118.
- Viveen W, Schoorl JM, Veldkamp A, van Balen RT. 2014. Modelling the impact of regional uplift and local tectonics on fluvial terrace preservation. *Geomorphology* **210**: 119–135. DOI:10.1016/j.geomorph.2013.12.026.
- Wainwright J. 2006. Degrees of separation: Hillslope-channel coupling and the limits of palaeohydrological reconstruction. *Catena* **66**(1–2): 93–106.
- Westaway R. 2004. Pliocene and Quaternary surface uplift evidenced by sediments of the Loire Allier river system (France). *Quaternaire* **15**: 103–115.
- Whittaker A, Boulton S. 2012. Tectonic and climatic controls on knick point retreat rates and landscape response times. *Journal of Geophysical Research* **117**: F02024. DOI:10.1029/2011JF002157.